THE JOURNAL OF BIOLOGICAL CHEMISTRY VOL. 292, NO. 3, pp. 884–897, January 20, 2017
Published in the U.S.A.

Identification of Hepatic Lysophosphatidylcholine Acyltransferase 3 as a Novel Target Gene Regulated by Peroxisome Proliferator-activated Receptor δ*

Received for publication, June 14, 2016, and in revised form, November 29, 2016 Published, JBC Papers in Press, December 2, 2016, DOI 10.1074/jbc.M116.743575

Amar Bahadur Singh and Jingwen Liu[1]

From the Department of Veterans Affairs Palo Alto Health Care System, Palo Alto, California 94304

Edited by John M. Denu

Peroxisome proliferator-activated receptor δ (PPARδ) regulates many genes involved in lipid metabolism. Hepatic lysophosphatidylcholine acyltransferase 3 (LPCAT3) has critical functions in triglycerides transport and endoplasmic reticulum stress response due to its unique ability to catalyze the incorporation of polyunsaturated fatty acids into phospholipids. Previous studies identified liver X receptor as the transcription factor controlling LPCAT3 expression in mouse liver tissue. Here we show that the hepatic *LPCAT3* gene is transcriptionally regulated by PPARδ. Adenovirus-mediated knockdown of PPARδ in cultured hepatic cells and liver tissue reduced LPCAT3 mRNA levels, and exogenous overexpression of PPARδ increased LPCAT3 mRNA expression. Activation of PPARδ in HepG2, Huh7, and Hepa 1-6 cells with its specific agonists increased LPCAT3 mRNA levels in all three hepatic cell lines. Through conducting sequence analysis, LPCAT3 promoter assays, and direct DNA binding assays, we have mapped the functional PPAR-responsive element to a proximal region from −135 to −123 of the LPCAT3 promoter that plays an essential role in mediating PPARδ-induced transactivation of the *LPCAT3* gene. Finally, we have provided *in vivo* evidence showing that activation of PPARδ by agonist L165041 in mice increased hepatic LPCAT3 mRNA abundance and LPCAT enzymatic activity, which is associated with increased incorporations of arachidonate into liver phosphatidylcholine and phosphatidylethanolamine. Furthermore, transient liver-specific knockdown of LPCAT3 in mice affected PPARδ-mediated activation of several hepatic genes involving in FA metabolism. Altogether, our new findings identify *LPCAT3* as a direct PPARδ target gene and suggest a novel function of PPARδ in regulation of phospholipid metabolism through LPCAT3.

Phospholipids (PLs)[2] are important components of biological membranes and also serve as precursors for the generation of diverse lipid signaling molecules. In mammalian cells, PLs are initially synthesized *de novo* and undergo further remodeling through deacylation by phospholipases and the subsequent reacylation by lysophospholipid acyltransferases (LPCATs). The LPCAT-dependent remodeling process is essential for the diversity and asymmetric distribution of acyl chains because the *de novo* PL synthesis pathway has poor substrate specificity (1). In the liver, LPCAT3 is the abundant isoform of the LPCAT family and catalyzes the formation of phosphatidylcholines (PCs) from saturated lyso-PCs and polyunsaturated fatty acids (PUFAs) at the *sn*-2 position (2). Recent new studies utilizing mouse models of liver-specific deletion of LPCAT3 revealed a critical role of LPCAT3 in very low density lipoprotein-triglyceride (VLDL-TG) secretion due to its unique ability to catalyze the incorporation of arachidonate into membranes (3). Mice lacking LPCAT3 in the liver show reduced plasma TGs and hepatosteatosis and secrete lipid-poor VLDL lacking arachidonoyl phospholipids. In another study, it was demonstrated that liver-specific overexpression of LPCAT3 reduces postprandial hyperglycemia and improves plasma lipoprotein metabolic profiles in mice fed a normal chow diet (4).

At the gene transcriptional level, a previous study identified liver X receptor (LXR) as the important transcription factor controlling LPCAT3 expression in liver tissue via an LXR response element (LXRE) in the proximal promoter region of the murine *Lpcat3* gene (5). It was further reported that the ligand-induced activation of LXR reduces hepatic inflammation and ER stress in hyperlipidemic mice through a LPCAT3-mediated mechanism.

The peroxisome proliferator-activated receptors (PPARs) belong to a subfamily of the nuclear receptor superfamily with three members: PPARδ (also called PPARβ), PPARα, and PPARγ (6). They are nutrition-sensitive transcription factors and regulate many genes with important functions in fatty acids (FAs) and glucose metabolism (7–9). PPARs contain a signature type II zinc finger DNA binding motif and a hydrophobic ligand binding domain. Upon activation by specific synthetic ligands (L165041, GW0742, WY14643, and 15d-PGJ2) (10) or endogenous ligands, including PUFAs (7), PPARs het-

* This work was supported by the Department of Veterans Affairs (Office of Research and Development, Medical Research Service) and by NCCIH, National Institutes of Health, Grant 1R01AT006336-01A1. The authors declare that they have no conflicts of interest with the contents of this article. The content is solely the responsibility of the authors and does not necessarily represent the official views of the National Institutes of Health.

[1] To whom correspondence should be addressed: VA Palo Alto Health Care System. 3801 Miranda Ave., Palo Alto, CA 94304. Tel.: 650-493-5000 (ext. 64411); Fax: 650-496-2505; E-mail: Jingwen.Liu@va.gov.

[2] The abbreviations used are: PL, phospholipid; LPCAT, lysophosphatidylcholine acyltransferase; PC, phosphatidylcholine; PUFA, polyunsaturated fatty acid; TG, triglyceride; LXR, liver X receptor; LXRE, LXR response element; PPAR, peroxisome proliferator-activated receptor; FA, fatty acid; RXR, retinoid X receptor; PPRE, PPAR response element; ACSL, long chain acyl-CoA synthetase; AA, arachidonic acid; ER, endoplasmic reticulum; qRT-PCR, quantitative RT-PCR; TSS, transcription start site; NEFA, nonesterified fatty acid; TC, total cholesterol; ESI, electrospray ionization; ANOVA, analysis of variance; MOI, multiplicity of infection; IFU, infectious unit.

erodimerize with retinoid X receptor (RXR) and subsequently bind to specific sequences on the DNA referred to the PPAR response element (PPRE) to activate the transcription of target genes encoding various enzymes with specific functions in PLs and FA metabolism.

One family of enzymes essential for FA metabolism in mammals is the long chain acyl-CoA synthetase (ACSL), which has five members, including ACSL1, ACSL3, ACSL4, ACSL5, and ACSL6 (11, 12). They catalyze the formation of fatty acyl-CoAs from ATP, CoA, and long chain fatty acids with certain degrees of substrate specificity (13, 14). In particular, ACSL4 has been shown to have marked substrate preference for PUFAs, including arachidonic acid (AA) (15). Recent *in vitro* studies further suggested that ACSL4 has specific functions in the AA incorporation into PLs (16, 17). Our previous studies conducted in hepatic cells and in liver tissue of hamsters have identified *ACSL4* as a direct target gene of PPARδ (18). Activation of PPARδ in liver cells led to increased ACSL4 protein abundance and higher arachidonyl-CoA synthetase activity, which could potentially provide more substrates to LPCAT3 as LPCAT3 synthesizes arachidonoyl-PC from AA-CoA and lyso-PCs (3, 19). Increases in LPCAT3 expression and activity are associated with the reduction of ER stress (5, 20). It has been widely recognized that ER stress is one underlying cause of metabolic diseases (21), and PPARδ activations prevent ER stress, inflammation, and insulin resistance in different metabolic tissues, including skeletal muscle and liver (22–26).

The aims of the current study are to determine whether LPCAT3 and ACSL4 are coordinately up-regulated by PPARδ and to further identify cis-acting elements in the regulatory region of the *LPCAT3* gene that mediate the induction of *LPCAT3* gene transcription by PPARδ agonists in hepatic cells.

Results

Hepatic Depletion of PPARδ Leads to the Suppression of LPCAT3 Gene Expression—To determine whether *LPCAT3* gene expression is directly regulated by PPARδ, we first made an Ad-shPPARδ adenoviral construct that expresses an shRNA targeting the human PPARδ coding sequence. HepG2 cells were transduced with Ad-shPPARδ or an shRNA control virus Ad-shLacZ for 3 days, and subsequently gene expression was analyzed by qRT-PCR. Fig. 1*A* shows that Ad-shPPARδ transduction specifically reduced PPARδ mRNA levels by nearly 90% compared with that in control cells transduced with Ad-shLacZ. Depletion of PPARδ significantly lowered LPCAT3 mRNA levels to ~64% of control ($p < 0.001$) and also reduced levels of *ACSL4* and *ACSL3* mRNA, both of which are known target genes of PPARδ. In contrast, expression of PPARδ shRNA in HepG2 cells did not diminish ACSL1 mRNA levels, which was consistent with our previous *in vivo* observations that PPARδ activation increased ACSL4 and ACSL3 expressions without affecting ACSL1 mRNA levels in hamster liver (18, 27).

Next, we transduced HepG2 cells with adenovirus expressing human PPARδ (Ad-PPARδ) or GFP (Ad-GFP). Transduced cells were treated with PPARδ agonist GW0742 or DMSO for 24 h (Fig. 1*B*). Gene expression analysis by qRT-PCR indicated that overexpression of PPARδ in HepG2 cells slightly but significantly increased LPCAT3 mRNA levels, which were further elevated by the PPARδ agonist to 2.4-fold of control of Ad-GFP-transduced cells without ligand treatment. We observed a similar pattern in elevation of ACSL4 mRNA levels by PPARδ overexpression and GW0742 treatment. To confirm the inducing effects of PPARδ agonists on *LPCAT3* gene expression in other hepatic cells, we treated HepG2, Huh7, and Hepa 1-6 cells with PPARδ-specific ligand L165041 and GW0742 (Fig. 1*C*). In all three liver cell lines, LPCAT3 mRNA levels were significantly elevated by both agonists, with L165041 being more potent. Thus, we treated HepG2 cells with different concentrations of L165041 and observed a dose-dependent increase in steady state expression of LPCAT3 and ACSL4 mRNA at 24 h after treatment of L165041 (Fig. 1, *D* and *E*). To examine the regulation of *LPCAT3* gene expression by PPARδ in liver tissue, we developed adenovirus (Ad-sh-mPPARδ) targeting mouse Pparδ and injected it into mice, and we also injected control mice with control virus Ad-shLacZ. After 10 days of viral infection, we quantified mRNA expressions of *Pparα*, *Pparδ*, *Pparγ*, and all *Lpcat* family members as well as several inflammatory genes from mouse liver tissues. Real-time PCR analysis revealed that, compared with Ad-shLacZ-infected control animals, Pparδ mRNA expression was reduced by ~62% ($p < 0.01$) in mice infected with the Ad-sh-mPPARδ adenovirus (Fig. 1*F*). Similar to results observed in cultured cells, this reduction in PPARδ was accompanied by a ~48% reduction in Lpcat3 mRNA expression ($p < 0.05$), whereas all other Lpcat mRNA levels were unchanged. Interestingly, knockdown of PPARδ expression resulted in elevations of inflammatory genes, including *Atf3*, *Chop*, and *Xbp1* in liver tissue. Altogether, these data demonstrate that *LPCAT3* gene expression is directly regulated by PPARδ along with ACSL4 in cultured hepatic cells and in liver tissue.

Mapping LPCAT3 Promoter to Identify PPARδ-responsive Cis-acting Elements—Utilizing the Matinspector software, we analyzed the upstream 5′-flanking region of the human *LPCAT3* gene to identify putative PPRE elements that may mediate the inducing effects of PPARδ agonists. Transcription factor prediction revealed the presence of two putative PPRE motifs within a 1-kb proximal promoter region that also contains the previously identified LXRE site (Fig. 2*A*). We designated these PPRE sites as PPRE1 and PPRE2. PPRE1 is located on the antisense strand of the promoter spanning the region −135 to −123 and is composed of two half-sites separated by a single nucleotide (3′-AGTGGAAACGGAA-5′). PPRE2 resides in the sense strand of the LPCAT3 promoter spanning the region −619 to −607. PPRE2 site is also a typical direct repeat 1 site (5′-AGGTCATGTTTTA-3′).

To assess the significance of these sequence motifs, we constructed a plasmid (pLPCAT3-Luc) containing the promoter region from −790 to +186 relative to the transcription start site (TSS) of the human *LPCAT3* gene (Fig. 2*A*). The inducing effects of the PPARδ ligands L165041 and GW0742 on the LPCAT3 promoter construct were examined in HepG2 cells along with a LXR-specific agonist GW3965 as comparator (5). PPARδ agonists and LXR agonist produced equivalent stimulating effects on the luciferase activity in HepG2 cells transfected with pLPCAT3-Luc (Fig. 2*B*), suggesting that *LPCAT3*

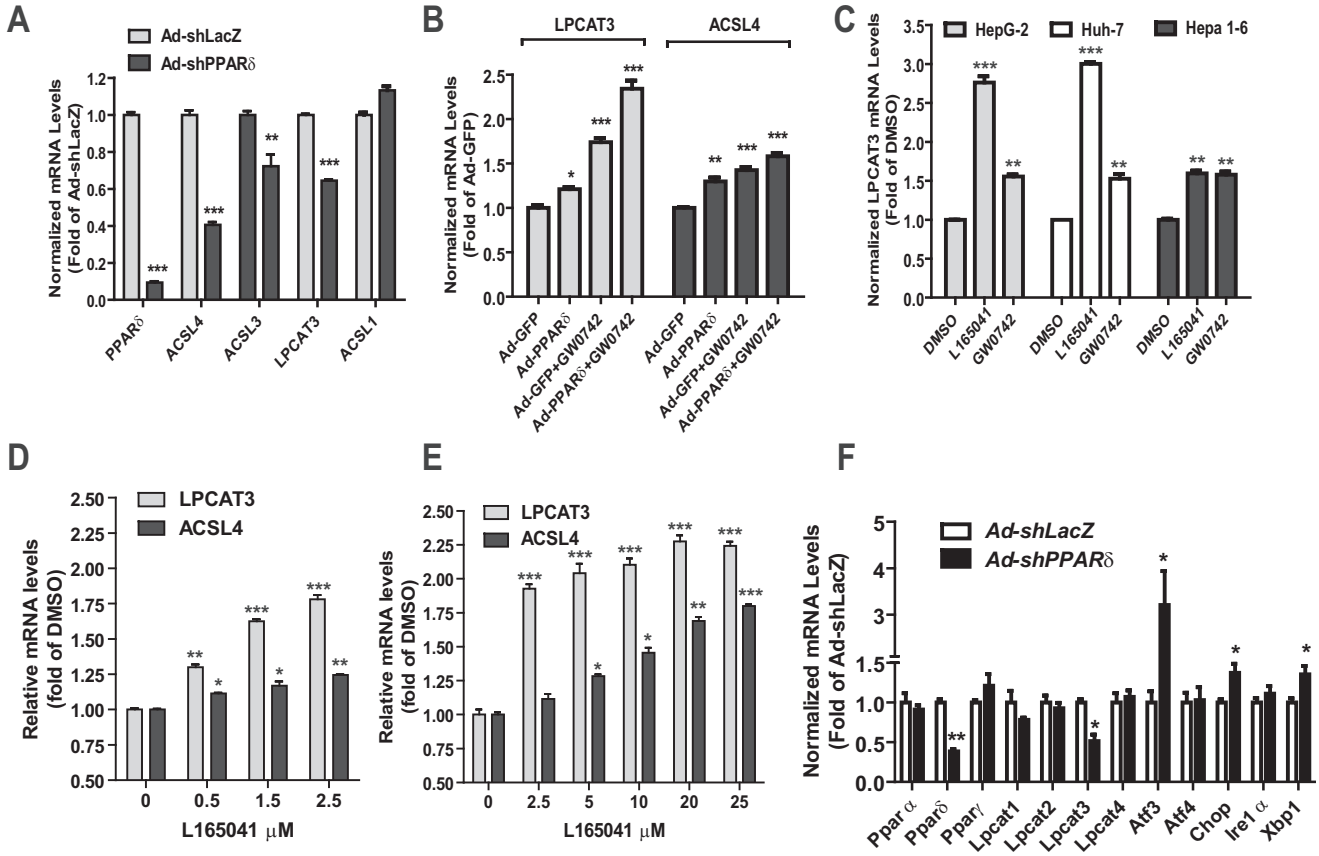

FIGURE 1. **Regulation of LPCAT3 mRNA expression by PPARδ activation.** *A*, HepG2 cells were seeded in a 12-well cell culture plate. After 24 h, cells were transduced with Ad-shLacZ (50 MOI) or Ad-shPPARδ (50 MOI) adenovirus in duplicate wells per transduction. Fresh cell culture medium was replaced 5 h later, and cells were incubated for a further 48 h. Total RNA was collected from transduced cells for quantitative PCR analysis. *Bars*, mean ± S.E. (*error bars*) of two RNA samples with triplicate measurement per RNA sample. **, $p < 0.01$; ***, $p < 0.001$. The data shown are representative of two independent assays. *B*, HepG2 cells were transduced with Ad-GFP (50 MOI) or Ad-PPARδ (50 MOI) adenoviruses in duplicate wells per transduction. Fresh cell culture medium was replaced 5 h later, and cells were incubated for a further 24 h and then subsequently treated with 1 μM GW0742 or DMSO. Total RNA was collected from transduced cells for quantitative PCR analysis. *Bars*, mean ± S.E. of two RNA samples with triplicate measurement per RNA sample. *, $p < 0.05$; **, $p < 0.01$; ***, $p < 0.001$. The data shown are representative of two independent assays. *C*, real-time PCR quantification of LPCAT3 mRNA expression from HepG2, Huh7, and Hepa 1-6 cells treated with GW0742 (1 μM), L165041 (20 μM), or DMSO for 24 h. LPCAT3 expression levels were normalized to GAPDH mRNA levels, where the relative expression of LPCAT3 mRNA in DMSO-treated cells was set at 1. *D* and *E*, qRT-PCR quantification of LPCAT3 or ACSL4 mRNA expression from HepG2 cells treated with L165041 at the indicated concentrations. *Bars*, mean ± S.E. of triplicate measurements of each RNA sample. The data shown are representative of two independent assays. *, $p < 0.05$; **, $p < 0.01$; ***, $p < 0.001$ compared with DMSO-treated samples. *F*, C57BL/6J mice fed a normal chow diet were injected with Ad-sh-mPPARδ ($n = 4$) or Ad-shLacZ ($n = 4$). Ten days after injection, mice were sacrificed for liver tissue collection. qRT-PCR was used to determine the relative expression levels (mean ± S.E., $n = 4$/group) of individual mRNAs after normalization with GAPDH mRNA levels. *, $p < 0.05$; **, $p < 0.001$, compared with the vehicle group, which was set at 1.

gene transcription is activated by PPARδ and LXR to similar extents. Next, we mutated the two PPRE sites individually and in combination on the wild type reporter pLPCAT3-Luc (Fig. 3*A*) and tested the response of mutated reporters to L165041 in Huh7 cells. Neither PPRE1 nor PPRE2 mutation affected basal promoter activity. Interestingly, the induction of LPCAT3 promoter activity by L165041 was not affected by disruption of the PPRE2 site; PPRE1 mutation, however, completely abolished the inducing activity of L165041 in Huh7 cells (Fig. 3*B*). Mutations of both PPRE1 and PPRE2 sites produced the same effects as PPRE1 mutation alone on LPCAT3 promoter activity. These results suggested that PPRE1 site is the functional regulatory sequence motif mediating PPARδ-induced transactivation of the *LPCAT3* gene. Next, we examined the individual effects of LXR agonist GW3965 and L165041 and their combination on the wild type promoter *versus* PPRE-mutated promoter activities (Fig. 3*C*). Treating cells with GW3965 and L165041 together produced an additive effect on the wild type LPCAT3 promoter activity. Ablation of the PPRE site did not significantly impact LXR activity but again abolished the PPARδ-mediated activation of LPCAT3 promoter activity, thereby suggesting the independent action of PPARδ and LXR on *LPCAT3* gene transcription.

Specific Interaction of PPARδ with PPRE1 Motif of LPCAT3 Promoter Is Enhanced by Ligand Treatment—PPARδ regulates gene transcription largely by forming heterodimers with RXRα and binding to PPRE motifs of its target genes. To determine whether the observed increase in LPCAT3 promoter activity by PPARδ agonist is directly attributed to PPARδ binding to the functional PPRE1 site under *in vitro* and *in vivo* conditions, we first examined the interaction of PPARδ with the LPCAT3-PPRE1 sequence by performing EMSA. Using biotin-labeled PPRE1 probe we demonstrated that the purified PPARδ-RXR heterodimers are capable of interacting with the biotinylated oligonucleotide probe encompassing the LPCAT3 promoter PPRE1 site (Fig. 4*A*, *lane 2*). Competition with wild type unla-

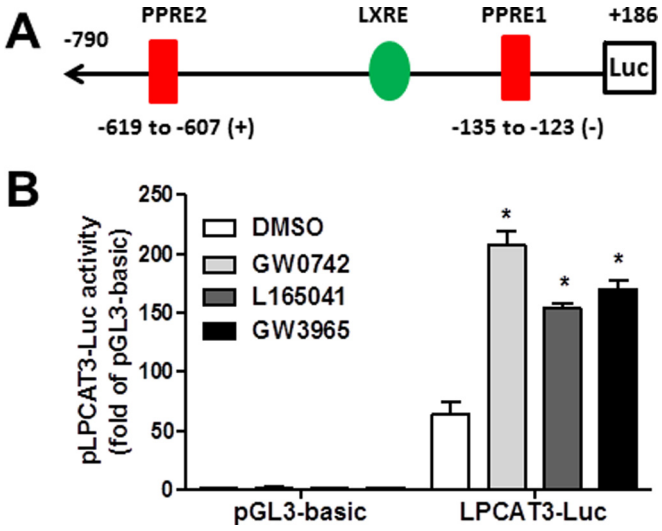

FIGURE 2. **Up-regulation of human LPCAT3 promoter activity in HepG2 cells by PPARδ agonists and LXR agonist.** *A*, diagrammatic representation of human LPCAT3 promoter luciferase reporter construct. *B*, relative luciferase activities from HepG2 cells transfected with pLPCAT3-Luc promoter luciferase plasmid or pGL3-basic vector. Data represent summarized results (mean ± S.E. (*error bars*)) of 4–6 replicates/treatment and are expressed as ratio of luciferase/β-gal activity from each sample, where the relative luminescence from cells transfected with promoterless pGL3-basic vector and treated with DMSO is set to 1. *, $p < 0.05$ compared with DMSO-treated samples. The data shown are representative of three separate transfection experiments.

beled probe resulted in almost complete quenching of the binding with the biotin-labeled probe (Fig. 4*A*, *lane 3*), whereas competition with an unlabeled probe harboring the mutant PPRE1 sequence were much less effective in repressing the binding of PPARδ-RXRα complex to the LPCAT3 promoter probe (Fig. 4*A*, *lane 4*). These results indicate that under *in vitro* conditions, PPARδ recognizes the PPRE1 sequence motif with high affinity and specificity.

To further assess the functional interaction of endogenous PPARδ with the LPCAT3 promoter in living cells with and without activation by an agonist, using a PPARδ-specific antibody, we performed a ChIP assay in HepG2 cells that were untreated or treated with L165041 at 10 and 20 μM concentrations. Compared with the control IgG antibody, we observed a higher immunoprecipitation of the LPCAT3 promoter region surrounding the PPRE1 site with anti-PPARδ antibody (Fig. 4*B*). Importantly, we detected a dose-dependent increase in the relative amount of LPCAT3 promoter immunoprecipitated by the PPARδ antibody after L165041 treatment. Furthermore, ChIP assays revealed very low binding of PPARδ to the PPRE2-LPCAT3 region regardless of ligand treatment. The ChIP results are highly corroborative with the functional assays of promoter activity that showed no effect of PPRE2 mutation on

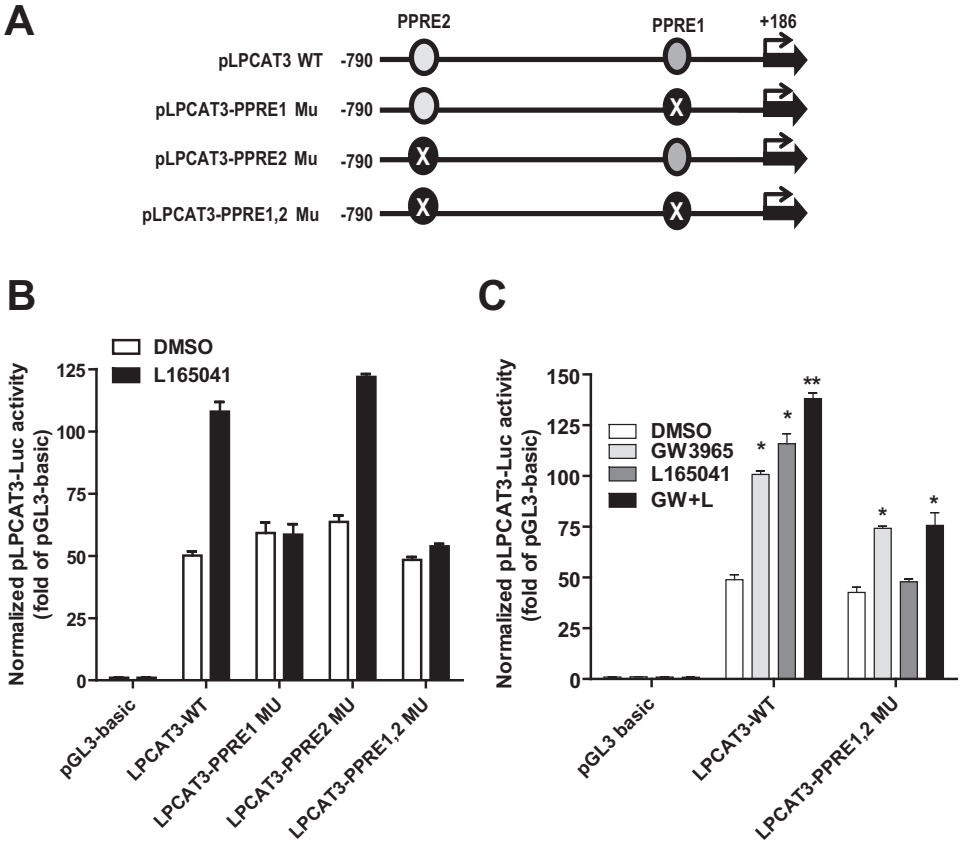

FIGURE 3. **Mapping the functional PPRE site in human LPCAT3 promoter.** *A*, diagrammatic representation of human LPCAT3 promoter luciferase reporter constructs of wild type and PPRE mutants. *B*, relative luciferase activities from control and L165041-treated Huh7 cells transfected with LPCAT3 promoter wild type and PPRE site-mutated reporter constructs or pGL3-basic vector. Data represent summarized results (mean ± S.E.) of 4 replicates/treatment and are expressed as the ratio of luciferase/β-gal activity from each sample. ***, $p < 0.001$ compared with DMSO-treated samples. *C*, after transfection, cells were treated with DMSO as control, 1 μM GW3965, 10 μM L165041, or GW3965 + L165041 for 24 h before cell lysis for the luciferase and β-gal activity assay. The graph represents relative luciferase activities from control and treated HepG2 cells transfected with LPCAT3 promoter wild type and PPRE site-mutated reporter constructs or pGL3-basic vector. Data represent summarized results (mean ± S.E. (*error bars*)) of 4 replicates/treatment and are expressed as the ratio of luciferase/β-gal activity from each sample. *, $p < 0.05$; ***, $p < 0.001$ compared with DMSO-treated samples. The data shown are representative of two separate transfection experiments.

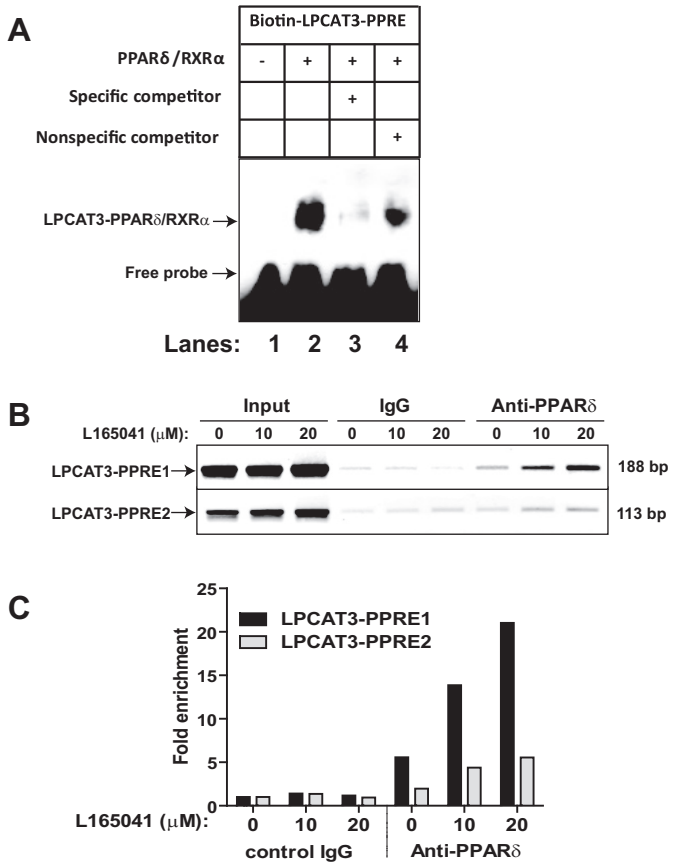

FIGURE 4. **EMSA and ChIP analyses of PPARδ association with PPRE1 site of LPCAT3 promoter *in vitro* and *in vivo*.** *A*, chemiluminescent signal from cross-linked nylon membrane, where biotin-5′-end-labeled LPCAT3-PPRE1 (*lanes 1–4*) was incubated with 200 ng of PPARδ and 100 ng of RXRα recombinant proteins in the absence (*lane 2*) or presence of a 100-fold molar excess of unlabeled wild type probe (*lane 3*) or mutated probe (*lane 4*). *B*, ChIP analysis on HepG2 cells treated with DMSO or L165041 (10 and 20 μM), where rabbit anti-PPARδ or isotype IgG antibody-immunoprecipitated DNA samples and input DNA samples were PCR-amplified with primers specific for the LPCAT3-PPRE1 and LPCAT3-PPRE2 promoter region. The PCR products were separated on a 2% agarose gel and stained with ethidium bromide. *C*, real-time quantitative PCR was performed using the two primer sets and chromatin DNA contained in the immunoprecipitates. Values from IgG-immunoprecipitated samples were arbitrarily set to 1.

LPCAT3 promoter activity. In addition, quantitative PCR was performed using the two primer sets and chromatin DNA contained in the immunoprecipitates. The results confirmed that L165041 treatment further increased the binding of PPARδ to the PPRE1 site in a dose-dependent manner (Fig. 4*C*). Altogether, these findings, for the first time, identify the *LPCAT3* gene as a novel target gene of PPARδ via a direct interaction of this nuclear receptor with the proximal PPRE1 motif of the human *LPCAT3* gene promoter.

Activation of PPARδ Increases Hepatic LPCAT3 and ACSL4 Expression in Mice—The aforementioned results established the important role of PPARδ as the trans-activator for *Lpcat3* gene transcription in hepatic cells. To examine whether this regulatory mechanism also operates in liver tissue *in vivo*, L165041 was orally administered to mice for 7 days at a daily dose of 40 mg/kg, whereas control mice received an equal volume of the vehicle. Measurement of serum lipid levels showed that L165041 treatment reduced serum TC levels by 14% ($p < 0.05$) and free FA (NEFA) levels by 17% ($p < 0.05$) as compared with control animals, whereas serum total PL levels were unchanged, and a trend in lowering TG was observed in L165041-treated mice (Fig. 5, *A–D*). We further performed HPLC separation of the pooled serum samples of control and L165041 treatment groups. Interestingly, although total serum TG showed a trend of reduction by L165041 treatment, HPLC analysis of lipoprotein-TG fractions revealed a 13% increase in VLDL-TG, whereas a 15% reduction in LDL-TG was detected (Fig. 5*E*). Further analysis of hepatic lipid levels showed a modest 13.1% ($p < 0.05$) reduction in cholesterol and a 20% ($p < 0.05$) reduction in FFA contents in the liver of L165041-treated mice compared with the vehicle group without a change in hepatic TG level (Fig. 5, *G–I*).

Utilizing qRT-PCR assays, we measured mRNA levels of all Lpcat family members in livers of control and L165041-treated mice. Fig. 6*A* shows that Lpcat3 is the most abundant isoform of this family, and it is the only enzyme being up-regulated by PPARδ ligand (Fig. 6*B*). These data provided *in vivo* evidence confirming the activating role of PPARδ in *Lpcat3* gene transcription. We tried to detect LPCAT3 protein in liver tissue by Western blotting with commercial available anti-LPCAT3 antibodies and failed to detect specific signals. The difficulty in detection of LPCAT3 protein has been previously reported in the literature (3). However, we measured the total LPCAT enzymatic activity in the liver microsomal fraction and detected a 44% increase by L165041 treatment (Fig. 6*C*). Further examinations of Acsl4 mRNA and protein levels in liver samples showed that Acsl4 mRNA levels were increased by 53% over control ($p < 0.001$) (Fig. 6*D*), and ACSL4 protein abundance was increased by 57% of control ($p < 0.001$) (Fig. 6*E*), thereby confirming the co-induction of Acsl4 with Lpcat3 in mice treated with L165041. In addition, we measured mRNA levels of a panel of genes involved in FA and cholesterol metabolism (Fig. 6*F*). The mRNA levels of *Cpt1α*, a marker gene for FA β-oxidation, were increased to 1.8-fold of control by L165041, consistent with the literature-reported activities of PPARδ on stimulating FA β-oxidation (28). Interestingly, the mRNA level of microsomal transport protein (Mttp) was also increased in L165041-treated mice. Because MTP is involved in the assembly of VLDL-TG in liver (29), the increase in MTP along with LPCAT3 may explain the increased serum level of the VLDL-TG fraction in mice treated with this PPARδ agonist.

Next, we applied a lipidomics approach to profile PC and PE molecular species in liver tissues of mice that were treated with L165041 or vehicle. Fig. 7*A* shows that arachidonoyl-PC (36:4, 16:0/18:4) was the most abundant PC species in liver tissue, and its level was increased by ~29% by L165041 treatment. Interestingly, we also detected increased incorporation of arachidonate and other PUFA into PE species PE (36:4, 16:0/18:4) and PE (38:6, 16:0/22:6) by PPARδ activation (Fig. 7*B*). These lipidomic data provided additional evidence for a direct effect of PPARδ activation on LPCAT3-mediated synthesis of arachidonoyl-PL species. Taken together, these data corroborated our *in vitro* findings of induction of *Lpcat3* gene expression by PPARδ activation and also demonstrated favorable plasma and hepatic lipid profiles with reductions in FFA and cholesterol levels in mice treated with PPARδ agonist.

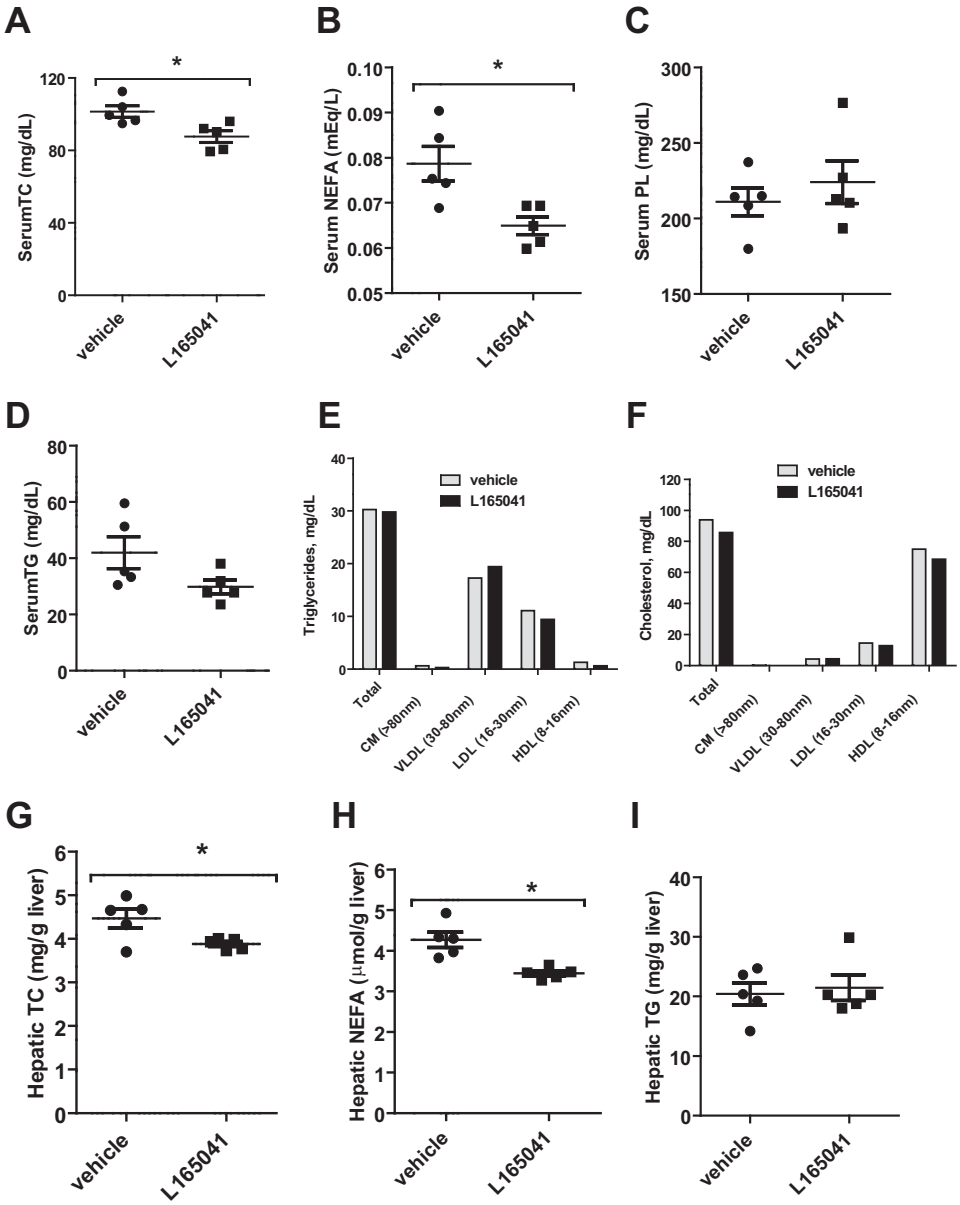

FIGURE 5. **Effects of PPARδ ligand treatment on serum and hepatic lipid levels of mice fed a normal chow diet.** Male C57BL/6J mice fed a chow diet were treated by daily gavage with vehicle ($n = 5$) or 40 mg/kg L165041 ($n = 5$) for 7 days. Four-h-fasted serum samples were collected 7 days after the initiation of drug treatment. Values are mean ± S.E. (*error bars*) of 5 mice/group. *A–D*, TC, NEFA, PL, and TG were measured from all serum samples. *, $p < 0.05$ compared with vehicle-treated serum samples. *E*, cholesterol distribution in HPLC-separated lipoprotein fractions from pooled serum samples of vehicle and L165041-treated mice. *F*, triglyceride distribution in HPLC-separated lipoprotein factions from pooled serum samples of vehicle and L165041-treated mice. *G–I*, lipids were extracted from individual liver samples, and TC, NEFA, and TG were measured. *, $p < 0.05$ as compared with the vehicle control group.

Liver-specific Lpcat3 Knockdown in Mice Affected PPARδ-mediated Activation of Hepatic Genes in FA Metabolic Pathway—To further understand the function of PPARδ in regulation of PL metabolism through the LPCAT3-ACSL4 pathway, we developed an adenovirus, Ad-shLPCAT3, to specifically knock down hepatic LPCAT3 expression in mice. Mice were injected with Ad-shLPCAT3 or Ad-shLacZ. Three days after viral injection, mice were treated with either L165041 (40 mg/kg) or vehicle for an additional 7 days. Measurement of liver LPCAT activity showed that Ad-shLPCAT3 infection reduced liver LPCAT activity by ~85% ($p < 0.001$) compared with that in Ad-shLacZ-infected mice (Fig. 8*A*), and L165041 treatment consistently increased LPCAT activity in the liver tissue of control mice (Fig. 8*B*). Hepatic gene expression analysis by qRT-PCR showed that the mRNA levels of Lpcat3 were significantly reduced in Ad-shLPCAT3-infected mice compared with control mice (Fig. 8*C*), which was in agreement with the enzyme assay results. Interestingly, the L165041-mediated elevations in Lpcat3, Acsl4, Mttp, and Cpt1α mRNA levels were not observed in mice infected with Ad-shLPCAT3. Depletion of LPCAT3 led to increased expression of stress genes *Atf3* and *Chop*, which have been observed in previous studies of mice with liver-specific Lpcat3 knockdown (5).

Measurements of serum and hepatic lipid levels showed that LPCAT3 depletion reduced serum TG (Fig. 9*A*) and elevated hepatic TG contents (Fig. 9*E*), which have been observed pre-

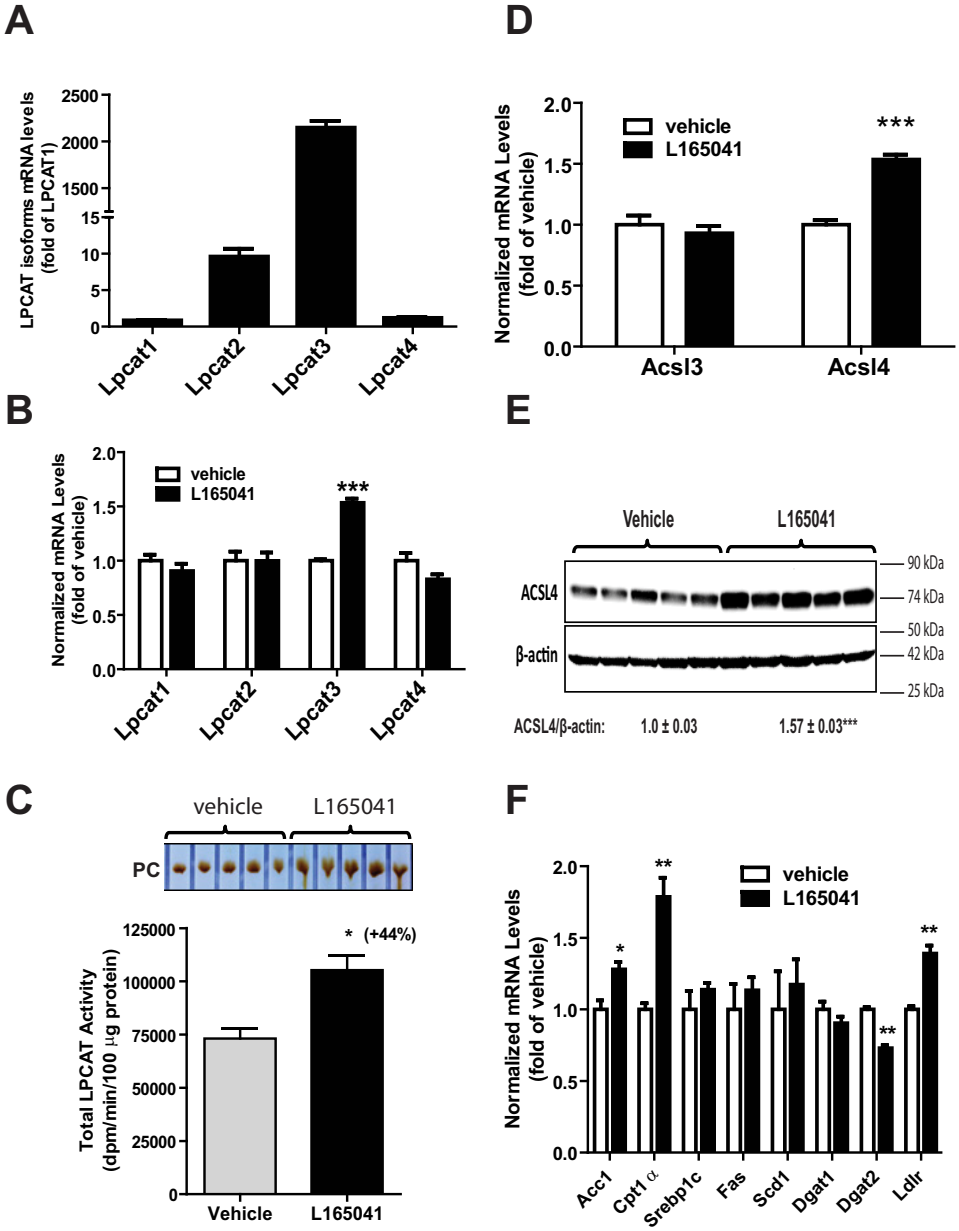

FIGURE 6. **Administering L165041 to mice increases hepatic Lpcat3 mRNA and LPCAT enzyme activity along with elevations of Acsl4 and other PPARδ-target genes.** Male C57BL/6 mice were gavaged daily with 40 mg/kg L165041 ($n = 5$) or vehicle ($n = 5$). After 7 days of treatment, the liver was excised, and the following were measured. *A*, all isoforms of Lpcat mRNAs. *B*, *D*, and *F*, qRT-PCR was conducted to determine the relative expression levels (mean ± S.E. (*error bars*), $n = 5$/group) of individual mRNAs after normalization with GAPDH mRNA levels. *, $p < 0.05$; **, $p < 0.01$; ***, $p < 0.001$, compared with the vehicle group, which was set at 1. *C*, total LPCAT activity (mean ± S.E., $n = 5$/group). ***, $p < 0.001$, compared with the control group. *E*, Western blotting analysis of hepatic ACSL4 protein levels.

viously in other animal models with genetic deletion of LPCAT3 (3). Activation of PPARδ by L165041 ameliorated the steatosis in Ad-LPCAT3-infected mice by lowering hepatic TG and hepatic TC (Fig. 9*F*) contents. Hepatic total PL contents were not changed by LPCAT3 depletion or L165041 treatment (Fig. 9*G*), whereas hepatic free FA (NEFA) levels were reduced by PPARδ activation (Fig. 9*H*) in both control and LPCAT3-depleted mice.

Serum TC levels were lower in L165041-treated mice regardless of LPCAT expression status (Fig. 9*B*). Recently, we have identified a PPRE regulatory motif in the LDLR promoter and demonstrated its functional role in activation of LDLR transcription independent of the SREBP pathway (30). Again, in this study, we observed increased LDLR mRNA levels in mice treated with L165041 (Fig. 8*C*); however, in contrast to *Acsl4* or other genes that are involved in FA and PL metabolism, the induction of LDLR by L165041 was independent of LPCAT3 expression levels. The reduction of serum TC is consistent with increased hepatic LDLR mRNA level in L165041-treated mice infected with Ad-shLPCAT3 or Ad-shLacZ.

Discussion

PPARδ activation in liver is known to activate a transcriptional program to increase cellular abundances of multiple

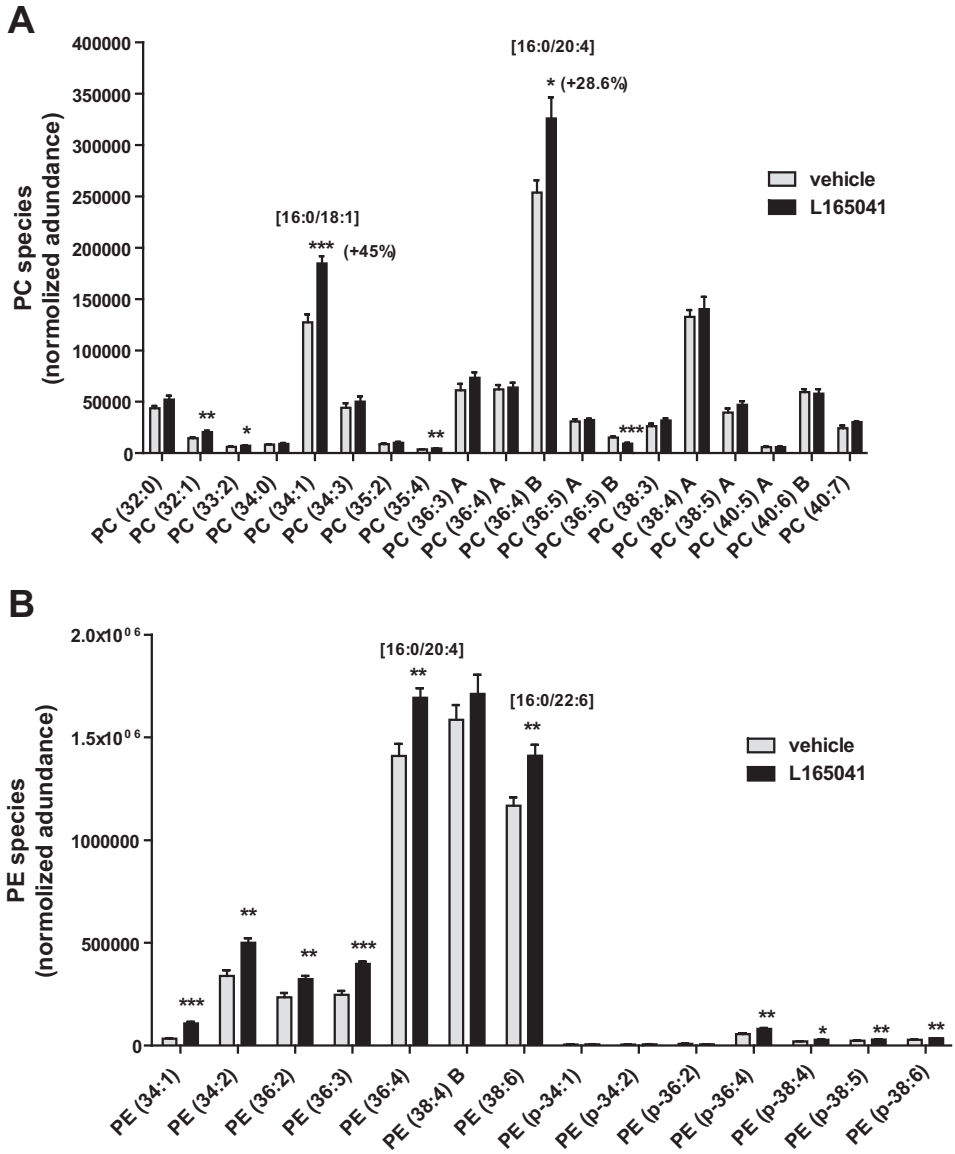

FIGURE 7. **Activation of PPARδ increases arachidonate into PCs and PEs in mouse liver.** CSH-ESI QTOF MS/MS analysis of the abundance of PC species in *A* and PE species in *B* in livers of chow-fed mice treated with L165041 or vehicle. Values are the mean ± S.E. (*error bars*) of 5 liver samples/group. *, $p < 0.05$; **, $p < 0.01$; ***, $p < 0.001$, compared with the vehicle group.

enzymes to modulate FA and PL metabolism (31). Our previous studies have identified ACSL4 as a new molecular target of PPARδ in liver cells (18). In this study, we explored the possibility that activation of PPARδ in liver tissue might not only increase ACSL4 cellular abundance and its enzymatic activity but could also affect the metabolic fates of ACSL4-produced PUFA-CoAs by altering the availability of ACSL4 fatty substrates, its interacting proteins, and downstream effectors. Because LPCAT3 synthesizes arachidonoyl-PC from lyso-PCs and PUFA-CoAs, in particular AA-CoA (3, 19), we focused our current study on examining the likelihood that LPCAT3 and ACSL4 are coordinately regulated by PPARδ to maximize the use of the AA-CoA in arachidonoyl-PC production. Now we have provided both *in vitro* and *in vivo* evidence demonstrating that, indeed, *LPCAT3* gene transcription is induced by PPARδ ligands along with ACSL4 in liver cells.

Utilizing adenovirus-mediated knockdowns in HepG2 cells and in mouse liver tissue, we showed that cellular depletion of PPARδ specifically reduced LPCAT3 mRNA levels, and conversely, overexpression of PPARδ was associated with increased *LPCAT3* gene expression. In our *in vitro* assays conducted in different hepatic cell lines, we demonstrated co-inductions of LPCAT3 with ACSL4 but not with ACSL1, the abundant isozyme of the ACSL family that has no substrate preference for arachidonate and predominately conjugates saturated FAs with CoAs (11).

To further demonstrate a direct effect of PPARδ on LPCAT3 transcription, we did a thorough sequence analysis of the 5′ upstream regulatory region of the *LPCAT3* gene and examined the potential involvements of two putative PPRE sequence motifs in the proximal region of the *LPCAT3* gene promoter. Our experimental results of a mutagenesis assay and *in vivo*

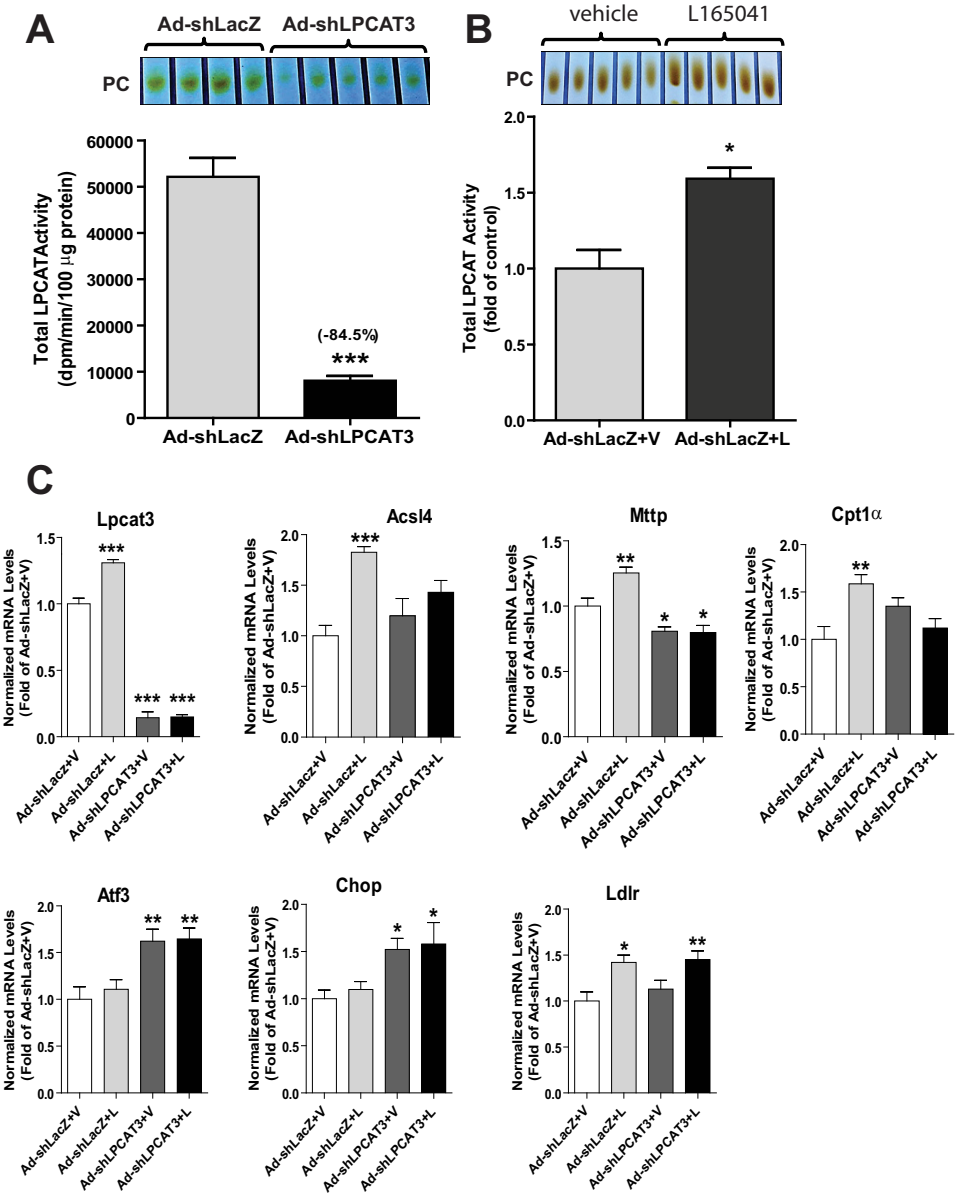

FIGURE 8. **Depletion of hepatic LPCAT3 expression in mice fed a chow diet attenuated PPARδ-mediated activation of hepatic genes in the FA metabolic pathway.** Male C57BL/6J mice ($n = 5$ animals/treatment) were retro-orbitally injected with 3×10^9 IFU/mouse of Ad-shLacZ or Ad-shLPCAT3 adenovirus particles. Three days after injection, mice were orally treated with L165041 (40 mg/kg) or vehicle for 7 days. Four-h-fasted serum samples were collected at the experimental termination, and the liver was excised for the total LPCAT activity assay (*A* and *B*) and gene expression analysis (*C*). Statistical analysis was performed using Student's *t* test for the enzyme assay (*A* and *B*), and one-way ANOVA with Dunnett post hoc test was performed in gene expression analysis. *, $p < 0.05$; **, $p < 0.01$; ***, $p < 0.001$, compared with the vehicle group injected with Ad-shLacZ. *V*, vehicle; *L*, L165041. *Error bars*, S.E.

DNA binding assays demonstrated that the binding of PPARδ to the PPRE1 site (−135 to −123) was induced by L165041 treatment in intact HepG2 cells, and disruption of this binding by altering the nucleotide sequence within this motif totally abolished the up-regulation of LPCAT3 promoter activity by PPARδ agonist. In contrast, the putative PPRE2 site (−619 to −607) was not bound by PPARδ *in vivo*, and disruption of the binding sequence had no impact on PPARδ-induced promoter activity, indicating that this putative motif is not a functional PPARδ binding site. Thus, our study identifies the proximal PPRE1 site as the authentic cis-acting element mediating the induction of *LPCAT3* gene transcription by PPARδ.

Numerous studies in different animal models have demonstrated the beneficial effects of PPARδ agonists in improving insulin sensitivity, reducing hyerlipidemia and hepatosteatosis through its multiple effects on anti-inflammation and reduction of ER stress (22–24, 28, 32). However, it has not been reported that LPCAT3 plays a role in the action of PPARδ, and there is no precedent report on PPARδ regulation of LPCAT3. In this study, we provided the first *in vivo* evidence that LPCAT3 expression and enzymatic activity in liver tissue are up-regulated by L165041, which may in some way contribute to the reduction of FFA levels in circulation as well as in the liver of normolipidemic mice. We did not observe changes in total PL levels in serum or in liver, which was in line with other studies showing that LPCAT3 depletion in liver did not affect total PL levels (3). However, our lipidomic analysis demonstrated higher abundances of arachidonoyl-PC species and PE species,

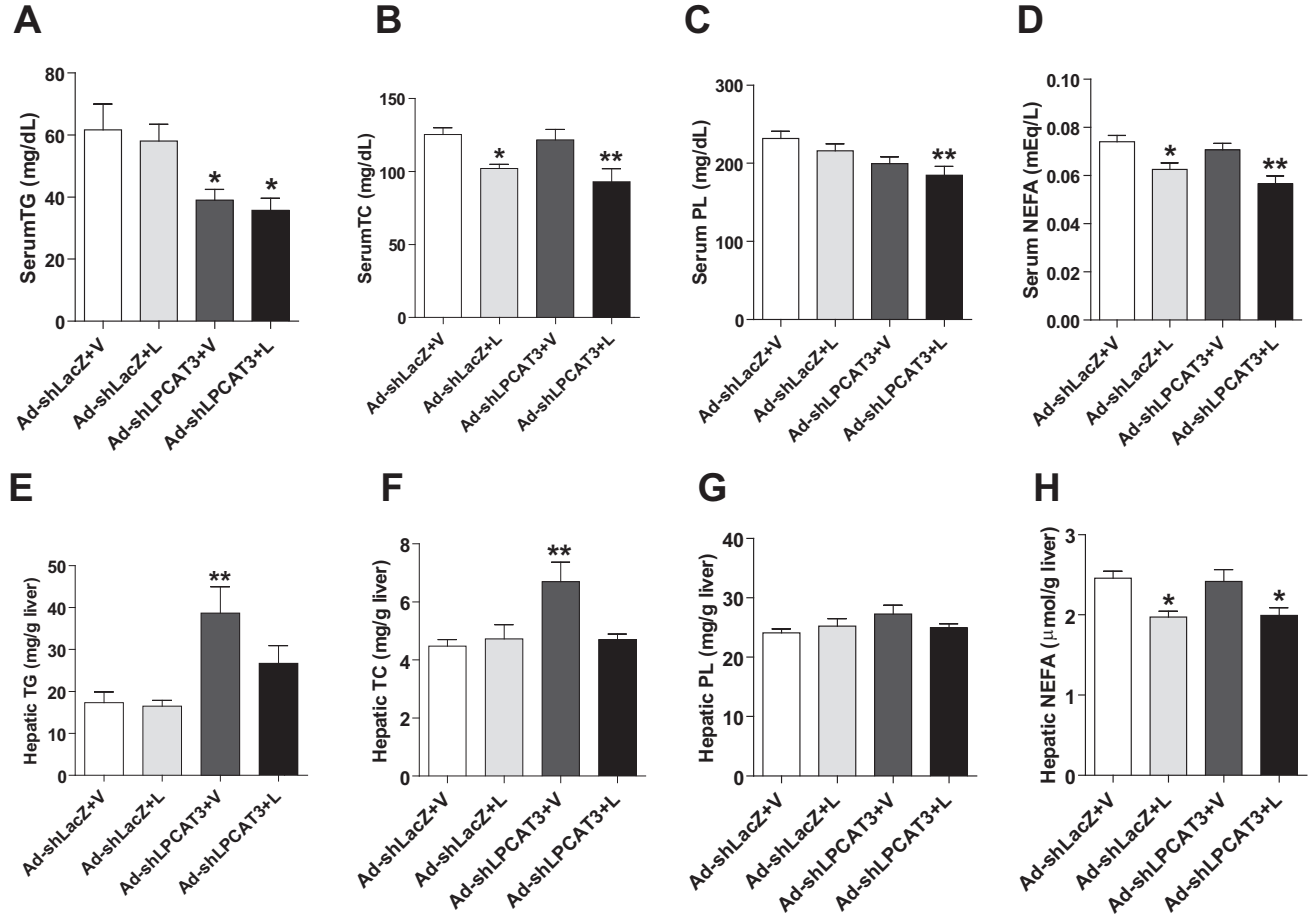

FIGURE 9. **Effects of hepatic LPCAT3 knockdown on serum and hepatic lipid levels of mice with or without L165041 treatment.** Male C57BL/6J mice (5 mice/group) were injected with 3×10^9 IFU/mouse of Ad-shLacZ or Ad-shLPCAT3 adenovirus particles. Three days after injection, mice were orally treated with L165041 (40 mg/kg) or vehicle for 7 days. Four-h-fasted serum samples were collected at the experimental termination, and the liver was excised. Serum TG (*A*), TC (*B*), PL (*C*), and NEFA (*D*) were measured. Liver lipids were extracted and used to measure hepatic TG (*E*), TC (*F*), PL (*G*), and NEFA (*H*). Statistical analysis was performed using one-way ANOVA with Dunnett's post hoc test. *, $p < 0.05$; **, $p < 0.01$; ***, $p < 0.001$, compared with the vehicle group injected with Ad-shLacZ. *V*, vehicle; *L*, L165041. *Error bars*, S.E.

in particular PC (36:4; 16:0/20:4) and PE (36:4; 16:0/20:4), in the liver of L165041-treated mice. This provides strong evidence to support a direct regulatory role of PPARδ in LPCAT3 expression. To further understand the function of LPCAT3 in the PPARδ-activated transcriptional program in liver tissue, we utilized adenovirus to transiently deplete liver LPCAT3 and examined responses of wild type mice and LPCAT3-depleted mice to L165041 treatment. Interestingly, we found that several PPARδ-regulated genes that encode enzymes involved in FA metabolism did not respond to PPARδ activation in Ad-shLPCAT3-infected mice. In contrast, induction of LDLR mRNA expression was not affected by knocking down LPCAT3. These new findings support our hypothesis that the LPCAT3/ACSL4 pathway is probably an integral part of a PPARδ-mediated transcriptional program.

In summary, previous studies have identified LXR as the trans-activator for *LPCAT3* gene expression in human macrophages (33) and mouse liver tissue (5). We now have demonstrated a new functional role of PPARδ in *LPCAT3* gene transcription in liver cells. We further show that, different from LXR agonist that has no effect on ACSL4 expression (34), PPARδ activation leads to coordinated up-regulation of LPCAT3 and ACSL4, consequently leading to an increased lysophosphatidylcholine acyltransferase enzyme activity. Our results suggest that the LPCAT3-ACSL4 axis has important roles in PPARδ-mediated amelioration of inflammation, ER stress, insulin resistance, and hepatosteatosis.

Experimental Procedures

Cells and Reagents—The human hepatoma cell lines HepG2 and Huh7 and mouse hepatoma cell line Hepa 1-6 were obtained from ATCC and cultured in Eagle's minimum essential medium and Dulbecco's modified Eagle's medium supplemented with 10% FBS (Thermo Fisher Scientific). PPARδ agonists L165041 and GW0742 were obtained from Tocris Bioscience. LXR agonist GW3965 and anti-β-actin monoclonal antibody were obtained from Sigma-Aldrich. Rabbit anti-ACSL4 antibody was reported previously (18). Rabbit anti-PPARδ antibody (sc-7197X) was obtained from Santa Cruz Biotechnology, Inc.

Constructions of Ad-shPPARδ Adenoviral Vector for PPARδ Knockdown in HepG2 Cells and in Mouse Liver—A U6 promoter-based vector (pSH-PPAR**δ**) that expresses an shRNA targeting human PPARδ coding region (5′-GCACATCTACAATGCCTACCT-3′) was generated using Invitrogen's BLOCK-iT™ U6 RNAi entry vector kit following the manufa-

TABLE 1
qRT-PCR primer, EMSA probes, promoter cloning primers, and ChIP primer sequences

Gene name	Forward	Reverse
Mouse primers		
Lpcat1	GTGCACGAGCTGCGACT	GCTGCTCTGGCTCCTTATCA
Lpcat2	TGTACTAATCGCTCCTGTTTGATT	CACTGGAACTCCTGGGATG
Lpcat3	GGCCTCTCAATTGCTTATTTCA	AGCACGACACATAGCAAGGA
Lpcat4	TTCGGTTTCAGAGGATACGACAA	AATGTCTGGATTGTCGGACTGAA
Acsl3	TCTTGCAAACAAAGCTGAAGGA	GGTTGGAGGCTTCCCATCAA
Acsl4	CTTCCTCTTAAGGCCGGGAC	TGCCATAGCGTTTTTCTTAGATTT
Acc1	AGCACAGCTCCAGATTGCCA	GGAGATACCCCATACATCATAC
Cpt1α	GGCCATCTGTGGGAGTATGT	ACTGTAGCCTGGTGGGTTTG
Srebp1c	CAAGGCCATCGACTACATCCG	CACCACTTCGGGTTTCATGC
Fas	GTGATAGCCGGTATGTCGGG	TAGAGCCCAGCCTTCCATCT
Scd1	CTGCAGGTTGTGCTAGATGGGATGG	GCCTGGGGTCTTTGGTAAGTAGGC
Dgat1	TGGTAGTGGGCCCAAGGTAG	GAATCTTGCAGACGATGGCAC
Dgat2	GGCTACGTTGGCTGGTAACT	TCTTCAGGGTGACTGCGTTC
Mttp	CCAGGGCTTTTGCCTTGAAC	GAGGACCTGTCCCACAATGG
Ldlr	ACCTGCCGACCTGATGAATTC	GCAGTCATGTTCACGGTCACA
Gapdh	ATGGTGAAGGTCGGTGTGAA	ACTGGAACATGTAGACCATGTAGT
Human primers		
LPCAT3	TGGGCCGCACCATCAC	AGTTGCCGGTGGCAGTGTA
PPARδ	AGCCAGTACAACCCACAGGT	CGATGTCGTGGATCACAAAG
ACSL1	CTTCTGGTACGCCACGAGAC	GTCGCTGTCAAGTAGTGCG
ACSL3	CCACGCCTGCGGCACATCAT	TGGTTTTCCATGCTGGCCTTGG
ACSL4	CCCTGAAGGATTTGAGATTCACA	CCTTAGGTCGGCCAGTAGAAC
GAPDH	ATGGGGAAGGTGAAGGTCG	GGGGTCATTGATGGCAACAATA
Human LPCAT3 promoter cloning primers		
LPCAT3 promoter WT	CCACGAGCTCGAGAATGAAAAGCAGGGAGG	GCAGCTCGAGGTTAAGGCTCAGCTCCTGG
LPCAT3-PPRE1 Mut.	TGCATTCTCGGCAGGAGTCACTCCCGCCTT ACAAACCTTCAGACCC	GGGTCTGAAGGTTTGTAAGGCGGGAGTGA CTCCTGCCGAGAATGCA
LPCAT3-PPRE2 Mut.	CATGCAGTTTCCTGTAGTAAAACATAGCTCT CCCCCTAGAGGCGATGAAATTAAG	CTTAATTTCATCGCCTCTAGGGGGAGAGC TATGTTTTACTACAGGAAACTGCATG
EMSA probes		
LPCAT3-PPRE1 WT	GCATTCTCGGCAGGAGTCACCTTTGCCTTA CAAACCTTCAGACCCGCC	GGCGGGTCTGAAGGTTTGTAAGGCAAAGGT GACTCCTGCCGAGAATGC
LPCAT3-PPRE1 Mut.	GCATTCTCGGCAGGAGTCACCCCCTCCTTA CAAACCTTCAGACCCGCC	GGCGGGTCTGAAGGTTTGTAAGGAGGG GGTGACTCCTGCCGAGAATGC
ChIP primers		
LPCAT3-PPRE1 (−37 to −225)	CGGGCTCAGACCTTTCCAAT	GCCAGCTCACCCCGTTATT
LPCAT3-PPRE2 (−539 to −652)	GGCATATCTTAATTTCATCGCCTCT	TGCCCCAGGAACAGACATTG

cturer's instruction. The sequence identity and orientation of PPARδ shRNA in pSH-PPARδ was confirmed by sequencing. The pSH-PPARδ plasmid was then recombined with pAD/BLOCK-iT DEST vector to generate Ad-shPPARδ viral vector and was transduced into HEK293A cells. The crude viral stocks were further amplified and purified. The titer of the purified virus was determined by the Adeno-X^{TM} rapid titer kit (Clontech). The viral titer was expressed as plaque-forming units (pfu/ml). Utilizing the same methods, an adenovirus (Ad-shmPPARδ) expressing an shRNA targeting the mouse PPARδ coding region (5′-GCAAGCCCTTCAGTGACATCA-3′) was generated for *in vivo* knockdown of PPARδ expression in mouse liver. An adenovirus expressing an shRNA targeting β-galactosidase was used as a control (Ad-shLacZ). In addition, purified adenoviral stocks expressing human PPARδ (Ad-GFP-PPARδ catalog no. 1284) and green fluorescent protein (Ad-GFP) (catalog no. 1060) were obtained from Vector Biolabs (Malvern, PA).

Constructions of Ad-shLPCAT3 Adenoviral Vector for LPCAT3 Knockdown in Mouse Liver—An adenovirus (Ad-sh-LPCAT3) expressing an shRNA targeting mouse LPCAT3 mRNA sequence (5′-GCCAATCTACTACGATTGTAT-3′) was generated and amplified by Vector Biolabs (Malvern, PA) for *in vivo* knockdown of LPCAT3 expression in mouse liver.

Adenoviral Transduction in Cell Culture—HepG2 cells were seeded at 5 × 10^5 cells/well in 12-well plates overnight. The next day, cells were transduced with the adenovirus at a multiplicity of infection (MOI) of 50 in 1 ml of medium containing 0.5% FBS for 5 h. Then medium containing virus was replaced by fresh medium containing 10% FBS. After 48 h of infection, cells were treated with PPARδ agonist, L165041 or GW0742, for 24 h, and then the cells were harvested for total RNA isolation and gene expression analysis.

Human LPCAT3 Promoter Cloning and PPRE Mutant Reporter Plasmid Construction—For generation of LPCAT3 promoter reporter, a DNA fragment of 977 bp covering the human LPCAT3 proximal promoter region from −790 to +186 relative to TSS was amplified from human genomic DNA (Promega) with a 5′-primer containing a SacI site and a 3′-primer containing an XhoI site. Gel-purified PCR product was digested with SacI and XhoI and subsequently cloned into the pGL3-basic luciferase vector (Promega). The PPRE mutant reporters were generated by using the LPCAT3 promoter plasmid as template and the QuikChange site-directed mutagenesis kit (Stratagene). The respective primer sequences and all other oligonucleotides used in this study are listed in Table 1. After transformation and propagation in *E. coli*, 3–6 independent clones per reporter construct were sequenced to verify the sequence and orientation of the promoter fragment.

Transfections and Luciferase Assay—The luciferase assay was performed as described previously (18). Briefly, HepG2 cells were seeded at a density of 3 × 10^4 cells/well onto 96-well

plates. The cells in each well were transfected with 100 ng of LPCAT3 promoter reporter plasmid and 10 ng of pCMV-β-gal plasmid as an internal control of transfection efficiency. Twenty-four h after transfection, cells were incubated with low serum (0.5% FBS) medium overnight and subsequently treated with PPARδ agonists for 24 h before cell lysis for both luciferase and β-galactosidase (β-gal) assays. Promoter luciferase activity was normalized by β-gal activity.

EMSA—EMSA was performed using the LightShift chemiluminescent EMSA kit (Pierce). Briefly, a 5′-end biotin-labeled probe identical to the 48-bp nucleotide region surrounding the putative PPRE1 element in the LPCAT3 promoter was synthesized. The DNA-protein binding assay was performed at room temperature for 20 min in a final volume of 20 μl with human recombinant proteins of PPARδ (200 ng) plus RXRα (100 ng) (Active Motif). The DNA-protein complexes were separated by 5% PAGE in 0.5× TBE buffer at 100 V for 1 h at room temperature and transferred to a Hybond-N nylon membrane (Amersham Biosciences). DNA-protein complexes were fixed to the membrane by a UV cross-linker (Bio-Rad), and biotin signal was detected using chemiluminescence. For competition experiments, a 100-fold higher concentration of unlabeled wild type or PPRE1 mutant oligonucleotide probe was incubated with the reaction mixture containing PPARδ/RXRα and biotin-LPCAT3 probe.

ChIP—The ChIP assay was conducted using Zymo-Spin™ ChIP kit (catalogue no. D5209, Zymo Research Corp., Irvine, CA) (34, 35). Briefly, HepG2 cells were seeded at a density of 3×10^6 cells/100-mm culture dish. The next day, cells were cultured in medium containing 0.5% FBS overnight and treated with PPARδ agonist L165041 or DMSO for 24 h. Cells were trypsinized, resuspended in PBS at a concentration of 6×10^6 cells/ml, and fixed with 1% formaldehyde (Sigma) for 10 min. To obtain nuclear lysates, fixed cells were resuspended in 500 μl of chromatin shearing buffer and sonicated at 4 °C in a Bioruptor 300 instrument (Diagenode, Inc.) for 13 cycles of 30 s on/30 s off at a high setting with intermittent vortex mixing. Chromatin-containing nuclear lysates (100 μl) were immunoprecipitated at 4 °C overnight with 5 μg of rabbit anti-PPARδ antibody (sc-7197X) or rabbit IgG as a negative control (Santa Cruz Biotechnology). Immunocomplexes were isolated by using protein A magnetic beads. ChIP DNA was eluted, cross-linking was reversed, and protein-free DNA was purified. The bound and the input DNA were analyzed by PCR with primers that amplify a 188-bp fragment of the human LPCAT3-PPRE1 promoter region −225 to −37 and a 113-bp fragment of LPCAT3-PPRE2 promoter region −652 to −539, relative to the TSS. The PCR conditions included a denaturation step at 94 °C for 3 min and then 31 cycles of 94 °C for 30 s, 55 °C for 30 s, 72 °C for 30 s, and extension at 72 °C for 7 min. The PCR products were visualized on a 2% agarose gel stained with ethidium bromide. Intensities of the PCR products were scanned and quantified with the Alpha View software (Cell Biosciences, Inc.). Additionally, real-time quantitative PCR was performed using the two primer sets and chromatin DNA contained in the immunoprecipitates. Primer sequences for the ChIP assay are listed in Table 1.

Animal Studies—Male C57BL/6J mice (8–10 weeks old) were purchased from Jackson Laboratory. Mice were fed a standard chow diet and housed under pathogen-free conditions in a temperature-controlled room with a 12-h light/dark cycle. Animals had free access to autoclaved water and food. All animal experiments were approved by and performed in accordance with the guidelines of the Veterans Affairs Palo Alto Health Care System Animal Care and Use Committee.

For the experiment of PPARδ activation, 10 mice were divided into two groups (5 mice/group) and were orally administered with PPARδ agonist L165041 at a daily dose of 40 mg/kg or vehicle (0.5% carboxymethyl cellulose) in 0.3 ml for 7 days. At the end of treatment, mice were fasted for 4 h. Blood samples were collected for the analysis of serum TC, TG, PL, and NEFA. Mice were sacrificed, and liver tissues were harvested and were snap-frozen in liquid nitrogen and stored at −80 °C until mRNA and protein extraction.

For the experiment of *in vivo* knockdown of hepatic PPARδ, eight mice were divided into two groups (4 mice/group). Group 1 was injected with adenovirus Ad-shLacZ (4×10^9 IFU/mouse), and the other group was injected with Ad-sh-mPPARδ (4×10^9 IFU/mouse). Ten days after adenovirus injection, mice were fasted for 4 h, and liver tissue samples were collected and stored at −80 °C for the analysis of mRNA expression.

For *in vivo* knockdown of LPCAT3, 20 mice were divided into four groups ($n = 5$). Mice were injected with Ad-shLacZ (3×10^9 IFU/mouse, groups 1 and 2) or Ad-shLPCAT3 (3×10^9 IFU/mouse, groups 3 and 4). Three days after injection, mice in group 1 and group 3 were orally administered with PPARδ agonist (L165041) at a daily dose of 40 mg/kg for 7 days, whereas mice in group 2 and 4 were gavaged with vehicle (0.5% carboxymethyl cellulose) for 7 days. At the end of the experiment, mice were fasted for 4 h, and blood samples were collected for serum lipid analysis. Livers were excised and snap-frozen in liquid nitrogen and stored at −80 °C for protein, mRNA, and lipid analyses.

Measurement of Serum and Hepatic Lipids—Blood was collected by retro-orbital bleeding, and the serum was separated by centrifugation. Serum and hepatic lipids were measured with the kit purchased from Stanbio Laboratory (Boerne, TX). The NEFA and phospholipid C measurement kit were purchased from Wako Diagnostics (Mountain View, CA). Hepatic lipids were extracted with the Folch lipid extraction method as we described previously (34) and measured with the same enzymatic kits.

HPLC Separation of Serum Lipoprotein Cholesterols and Triglycerides—After 7 days of treatment, individual fasting serum samples from the L165041-treated group and vehicle control group were pooled together to analyze cholesterol and triglyceride levels of each of the major lipoprotein classes, including chylomicron (>80 mm), VLDL (30–80 nm), LDL (16–30 nm), and HDL (8–16 nm) with a dual detection HPLC system consisting of two tandem connected TSKgel Lipopropak XL columns (300 × 7.8 mm; Tosoh, Tokyo, Japan) at Skylight Biotech, Inc. (Tokyo, Japan) as we described previously (36).

Isolation of Total RNA and qRT-PCR—Total RNA was isolated from 20 mg of flash-frozen liver tissue samples or from treated hepatic cells by using an RNeasy Plus minikit (Qiagen) or Quick RNA kit (Zymo Research). Complementary DNA syn-

thesis was carried out using SuperScript III reverse transcriptase (Life Technologies) and 2 μg of total RNA as a template. Quantitative real-time PCR was performed using SYBR Green Master Mix and an ABI 7900HT sequence detection system (Applied Biosystems) and PCR primers specific for each gene being amplified. Target mRNA expression in each sample was normalized to the housekeeping gene *GAPDH*. The $2^{-\Delta\Delta Ct}$ method was used to calculate relative mRNA expression levels.

Liver Membrane (Microsomal) Protein Isolation and LPCAT Activity Assay—For microsomal protein isolation, 100 mg of liver tissue were homogenized in homogenization buffer containing 100 mM Tris-HCl, pH 7.4, 2 mM EDTA, 300 mM sucrose, and complete protease inhibitor. Homogenate were centrifuged at 1000 $\times$ *g* for 10 min, and supernatants were further subjected to ultracentrifugation at 100,000 $\times$ g for 1 h. Thereafter, pellets were resuspended in homogenization buffer. Protein concentrations were estimated by the BCA protein assay kit. LPCAT enzyme activity was determined by measuring the incorporation of radiolabeled acyl-CoA into phospholipids as described previously (19). In brief, the reaction mixture in a total volume of 100 μl contained 100 mM Tris-HCl, pH 7.4, 2 mM EDTA, 300 mM sucrose, 2 mM $CaCl_2$, 0.015% Tween 20, 1 mg/ml fatty acid-free bovine serum albumin, 200 μM 16:0 lyso-PC (Avanti Polar Lipids), 20 μM [1-^{14}C]arachidonyl-CoA (American Radiochemicals), and 100 μg of liver membrane proteins. The reaction was initiated by the addition of the membrane proteins, incubated for 20 min at room temperature, and stopped by adding 375 μl of chloroform/methanol (1:2, v/v). Phospholipids were extracted by the method of Bligh and Dyer. The organic phase was dried under nitrogen gas. Lipids were redissolved in 30 μl of chloroform and then applied onto silica gel H plates (catalog no. 10011, Anatech, Newark, DE) along with PC standard. The running solvent for quantifying individual phospholipid classes was chloroform/methanol/glacial acetic acid/water, 60:50:1:4 (2). After separation and drying off the solvent, lipids were visualized by iodine vapor. The PC spots were scraped off the plate, and the ^{14}C radioactivity in the spots was measured by scintillation counting.

Lipidomics—Fifty mg of individual frozen liver samples from mice treated with L165041 ($n = 5$) or vehicle ($n = 5$) were subjected to lipidomic analysis at the West Coast Metabolic Center (University of California, Davis, CA). Five replicas of extracted lipids from each treatment group were applied to the lipidomics study using an automated electrospray ionization-tandem mass spectrometry (ESI-MS/MS) approach with a group of internal lipid standards. The LC/MS/MS analyses were carried out on an Agilent 1200 SL UHPLC system (Santa Clara, CA) coupled with an AB Sciex 4000 QTRAP system (Foster City, CA) under negative MRM mode. The detailed methods were described previously (37). The specific peaks on the spectra are normalized and are relative semiquantifications. All data acquisition, analysis, acyl group identification, and normalization were conducted by the West Coast Metabolic Center.

Statistical Analysis—Statistics were performed using Student's *t* test (two groups) or one-way ANOVA (more than two groups), with Dunnett's post hoc test to compare with the control group. Data are presented as means $\pm$ S.E., as indicated, and considered statistically significant at $p < 0.05$.

Author Contributions—A. B. S. performed *in vitro* and *in vivo* experiments and contributed to the manuscript writing. J. L. conceived and coordinated the study and wrote the paper. Both authors reviewed the results and approved the final version of the manuscript.

Acknowledgment—We thank Dr. Tomomi Hashidate-Yoshida (Department of Lipid Signaling, National Center for Global Health and Medicine, Tokyo, Japan) for providing technical help in Western blotting of liver LPCAT3.

References

1. Yamashita, A., Hayashi, Y., Nemoto-Sasaki, Y., Ito, M., Oka, S., Tanikawa, T., Waku, K., and Sugiura, T. (2014) Acyltransferases and transacylases that determine the fatty acid composition of glycerolipids and the metabolism of bioactive lipid mediators in mammalian cells and model organisms. *Prog. Lipid Res.* **53,** 18–81
2. Zhao, Y., Chen, Y. Q., Bonacci, T. M., Bredt, D. S., Li, S., Bensch, W. R., Moller, D. E., Kowala, M., Konrad, R. J., and Cao, G. (2008) Identification and characterization of a major liver lysophosphatidylcholine acyltransferase. *J. Biol. Chem.* **283,** 8258–8265
3. Rong, X., Wang, B., Dunham, M. M., Hedde, P. N., Wong, J. S., Gratton, E., Young, S. G., Ford, D. A., and Tontonoz, P. (2015) Lpcat3-dependent production of arachidonoyl phospholipids is a key determinant of triglyceride secretion. *elife* **4,** e06557
4. Cash, J. G., and Hui, D. Y. (2016) Liver-specific overexpression of LPCAT3 reduces postprandial hyperglycemia and improves lipoprotein metabolic profile in mice. *Nutr. Diabetes* **6,** e206
5. Rong, X., Albert, C. J., Hong, C., Duerr, M. A., Chamberlain, B. T., Tarling, E. J., Ito, A., Gao, J., Wang, B., Edwards, P. A., Jung, M. E., Ford, D. A., and Tontonoz, P. (2013) LXRs regulate ER stress and inflammation through dynamic modulation of membrane phospholipid composition. *Cell Metab.* **18,** 685–697
6. Schmidt, A., Endo, N., Rutledge, S. J., Vogel, R., Shinar, D., and Rodan, G. A. (1992) Identification of a new member of the steroid hormone receptor superfamily that is activated by a peroxisome proliferator and fatty acids. *Mol. Endocrinol.* **6,** 1634–1641
7. Lee, C., Olson, P., and Evans, R. M. (2003) Mini review: Lipid metabolism, metabolic diseases, and peroxisome proliferator-activated receptors. *Endocrinology* **144,** 2201–2207
8. Liu, S., Hatano, B., Zhao, M., Yen, C. C., Kang, K., Reilly, S. M., Gangl, M. R., Gorgun, C., Balschi, J. A., Ntambi, J. M., and Lee, C. H. (2011) Role of peroxisome proliferator-activated receptor δ/β in hepatic metabolic regulation. *J. Biol. Chem.* **286,** 1237–1247
9. Michalik, L., Auwerx, J., Berger, J. P., Chatterjee, V. K., Glass, C. K., Gonzalez, F. J., Grimaldi, P. A., Kadowaki, T., Lazar, M. A., O'Rahilly, S., Palmer, C. N., Plutzky, J., Reddy, J. K., Spiegelman, B. M., Staels, B., and Wahli, W. (2006) International Union of Pharmacology. LXI. Peroxisome proliferator-activated receptors. *Pharmacol. Rev.* **58,** 726–741
10. Sznaidman, M. L., Haffner, C. D., Maloney, P. R., Fivush, A., Chao, E., Goreham, D., Sierra, M. L., LeGrumelec, C., Xu, H. E., Montana, V. G., Lambert, M. H., Willson, T. M., Oliver, W. R., Jr., and Sternbach, D. D. (2003) Novel selective small molecule agonists for peroxisome proliferator-activated receptor delta (PPARδ) synthesis and biological activity. *Bioorg. Med. Chem. Lett.* **13,** 1517–1521
11. Soupene, E., and Kuypers, F. A. (2008) Mammalian long-chain acyl-CoA synthetases. *Exp. Biol. Med.* **233,** 507–521
12. Lopes-Marques, M., Cunha, I., Reis-Henriques, M. A., Santos, M. M., and Castro, L. F. (2013) Diversity and history of the long-chain acyl-CoA synthetase (Acsl) gene family in vertebrates. *BMC Evol. Biol.* **13,** 271
13. Grevengoed, T. J., Klett, E. L., and Coleman, R. A. (2014) Acyl-CoA metabolism and partitioning. *Annu. Rev. Nutr.* **34,** 1–30

14. Mashek, D. G., Li, L. O., and Coleman, R. A. (2007) Long-chain acyl-CoA synthetases and fatty acid channeling. *Future Lipidol.* **2,** 465–476
15. Kang, M. J., Fujino, T., Sasano, H., Minekura, H., Yabuki, N., Nagura, H., Iijima, H., and Yamamoto, T. T. (1997) A novel arachidonate-preferring acyl-CoA synthetase is present in steroidogenic cells of the rat adrenal, ovary, and testis. *Proc. Natl. Acad. Sci. U.S.A.* **94,** 2880–2884
16. Kuwata, H., Yoshimura, M., Sasaki, Y., Yoda, E., Nakatani, Y., Kudo, I., and Hara, S. (2014) Role of long-chain acyl-coenzyme A synthetases in the regulation of arachidonic acid metabolism in interleukin 1β-stimulated rat fibroblasts. *Biochim. Biophys. Acta* **1841,** 44–53
17. Küch, E. M., Vellaramkalayil, R., Zhang, I., Lehnen, D., Brügger, B., Sreemmel, W., Ehehalt, R., Poppelreuther, M., and Füllekrug, J. (2014) Differentially localized acyl-CoA synthetase 4 isoenzymes mediate the metabolic channeling of fatty acids towards phosphatidylinositol. *Biochim. Biophys. Acta* **1841,** 227–239
18. Kan, C. F., Singh, A. B., Dong, B., Shende, V. R., and Liu, J. (2015) PPARδ activation induces hepatic long-chain acyl-CoA synthetase 4 expression *in vivo* and *in vitro*. *Biochim. Biophys. Acta* **1851,** 577–587
19. Hashidate-Yoshida, T., Harayama, T., Hishikawa, D., Morimoto, R., Hamano, F., Tokuoka, S. M., Eto, M., Tamura-Nakano, M., Yanobu-Takanashi, R., Mukumoto, Y., Kiyonari, H., Okamura, T., Kita, Y., Shindou, H., and Shimizu, T. (2015) Fatty acid remodeling by LPCAT3 enriches arachidonate in phospholipid membranes and regulates triglyceride transport. *Elife* 10.7554/eLife.06328
20. Sun, X., Haas, M. E., Miao, J., Mehta, A., Graham, M. J., Crooke, R. M., Pais de Barros, J. P., Wang, J. G., Aikawa, M., Masson, D., and Biddinger, S. B. (2016) Insulin dissociates the effects of liver X receptor on lipogenesis, endoplasmic reticulum stress, and inflammation. *J. Biol. Chem.* **291,** 1115–1122
21. Gao, S., Han, X., Fu, J., Yuan, X., Sun, X., and Li, Q. (2012) Influence of chronic stress on the compositions of hepatic cholesterol and triglyceride in male Wistar rats fed a high fat diet. *Hepatol. Res.* **42,** 686–695
22. Coll, T., Rodrïguez-Calvo, R., Barroso, E., Serrano, L., Eyre, E., Palomer, X., and Vázquez-Carrera, M. (2009) Peroxisome proliferator-activated receptor (PPAR) β/δ: a new potential therapeutic target for the treatment of metabolic syndrome. *Curr. Mol. Pharmacol.* **2,** 46–55
23. Wagner, K. D., and Wagner, N. (2010) Peroxisome proliferator-activated receptor β/δ (PPARβ/δ) acts as regulator of metabolism linked to multiple cellular functions. *Pharmacol. Ther.* **125,** 423–435
24. Salvadó, L., Serrano-Marco, L., Barroso, E., Palomer, X., and Vázquez-Carrera, M. (2012) Targeting PPARβ/δ for the treatment of type 2 diabetes mellitus. *Expert Opin. Ther. Targets* **16,** 209–223
25. Salvadó, L., Barroso, E., Gómez-Foix, A. M., Palomer, X., Michalik, L., Wahli, W., and Vázquez-Carrera, M. (2014) PPARβ/δ prevents endoplasmic reticulum stress-associated inflammation and insulin resistance in skeletal muscle cells through an AMPK-dependent mechanism. *Diabetologia* **57,** 2126–2135
26. Ramirez, T., Tong, M., Chen, W. C., Nguyen, Q. G., Wands, J. R., and de la Monte, S. M. (2013) Chronic alcohol-induced hepatic insulin resistance and endoplasmic reticulum stress ameliorated by peroxisome-proliferator activated receptor-δ agonist treatment. *J. Gastroenterol. Hepatol.* **28,** 179–187
27. Cao, A., Li, H., Zhou, Y., Wu, M., and Liu, J. (2010) Long chain acyl-CoA synthetase-3 is a molecular target for peroxisome proliferator-activated receptor δ in HepG2 hepatoma cells. *J. Biol. Chem.* **285,** 16664–16674
28. Liu, S., Brown, J. D., Stanya, K. J., Homan, E., Leidl, M., Inouye, K., Bhargava, P., Gangl, M. R., Dai, L., Hatano, B., Hotamisligil, G. S., Saghatelian, A., Plutzky, J., and Lee, C. H. (2013) A diurnal serum lipid integrates hepatic lipogenesis and peripheral fatty acid use. *Nature* **502,** 550–554
29. Wierzbicki, A. S., Hardman, T., and Prince, W. T. (2009) Future challenges for microsomal transport protein inhibitors. *Curr. Vasc. Pharmacol.* **7,** 277–286
30. Shende, V. R., Singh, A. B., and Liu, J. (2015) A novel peroxisome proliferator response element modulates hepatic low-density lipoprotein receptor gene transcription in response to PPARδ activation. *Biochem. J.* **472,** 275–286
31. Chehaibi, K., Cedó, L., Metso, J., Palomer, X., Santos, D., Quesada, H., Naceur Slimane, M., Wahli, W., Julve, J., Vázquez-Carrera, M., Jauhiainen, M., Blanco-Vaca, F., and Escolà-Gil, J. C. (2015) PPAR-β/δ activation promotes phospholipid transfer protein expression 6. *Biochem. Pharmacol.* **94,** 101–108
32. Bojic, L. A., Telford, D. E., Fullerton, M. D., Ford, R. J., Sutherland, B. G., Edwards, J. Y., Sawyez, C. G., Gros, R., Kemp, B. E., Steinberg, G. R., and Huff, M. W. (2014) PPARδ activation attenuates hepatic steatosis in $Ldlr^{-/-}$ mice by enhanced fat oxidation, reduced lipogenesis, and improved insulin sensitivity. *J. Lipid Res.* **55,** 1254–1266
33. Ishibashi, M., Varin, A., Filomenko, R., Lopez, T., Athias, A., Gambert, P., Blache, D., Thomas, C., Gautier, T., Lagrost, L., and Masson, D. (2013) Liver X receptor regulates arachidonic acid distribution and eicosanoid release in human macrophages: a key role for lysophosphatidylcholine acyltransferase 3. *Arterioscler. Thromb. Vasc. Biol.* **33,** 1171–1179
34. Dong, B., Kan, C. F., Singh, A. B., and Liu, J. (2013) High-fructose diet downregulates long-chain acyl-CoA synthetase 3 expression in liver of hamsters via impairing LXR/RXR signaling pathway. *J. Lipid Res.* **54,** 1241–1254
35. Singh, A. B., Kan, C. F., Dong, B., and Liu, J. (2016) SREBP2 activation induces hepatic long-chain acyl-CoA synthetase 1 expression *in vivo* and *in vitro* through a SRE motif of ACSL1 C-promoter. *J. Biol. Chem.* **291,** 5373–5384
36. Dong, B., Singh, A. B., Fung, C., Kan, K., and Liu, J. (2014) CETP inhibitors downregulate hepatic LDL receptor and PCSK9 expression *in vitro* and *in vivo* through a SREBP2 dependent mechanism. *Atherosclerosis* **235,** 449–462
37. Yang, J., Solaimani, P., Dong, H., Hammock, B., and Hankinson, O. (2013) Treatment of mice with 2,3,7,8-tetrachlorodibenzo-*p*-dioxin markedly increases the levels of a number of cytochrome P450 metabolites of ω-3 polyunsaturated fatty acids in the liver and lung. *J. Toxicol. Sci.* **38,** 833–836